MR angiography of aneurysm models of various shapes and neck sizes.

H Isoda, R G Ramsey, Y Takehara, M Takahashi and M Kaneko

AJNR Am J Neuroradiol 1997, 18 (8) 1463-1472
http://www.ajnr.org/content/18/8/1463

MR Angiography of Aneurysm Models of Various Shapes and Neck Sizes

Haruo Isoda, Ruth G. Ramsey, Yasuo Takehara, Motoichiro Takahashi, and Masao Kaneko

PURPOSE: To investigate the signal intensity of lateral and terminal saccular aneurysm models with differing neck sizes using three-dimensional time-of-flight (TOF) MR angiography with various imaging parameters. **METHODS:** The study included four lateral and four terminal saccular aneurysm models with pulsatile flow. The height and fundus diameter were 10 mm; the neck diameters were 2.5 mm, 5 mm, 7.5 mm, and 10 mm, respectively. Each aneurysm model was examined wit h fast imaging with steady-state precession MR sequences with parameters of 20–140/7 (repetition time/echo time) and flip angles of 10° to 30°. Signal intensity was measured and compared among the models. **RESULTS:** Three-dimensional TOF MR angiography with the shorter repetition time and/or larger flip angle showed weaker signal intensity in the aneurysm models. Stronger signal intensity was obtained in the terminal saccular aneurysm models and/or the models with a wider neck than in the lateral saccular aneurysm models and/or the models with a narrower neck. In some aneurysm models, longer repetition times produced greater signal intensity than that of background brain models, but not in aneurysms with narrow necks. **CONCLUSION:** Noncontrast 3-D TOF MR angiography delineated terminal saccular aneurysms and/or aneurysms with wider necks and did not delineate lateral saccular aneurysms and/or aneurysms with narrower necks. Longer repetition times are recommended to allow the spins flowing into the aneurysms to recover.

Index terms: Aneurysm, magnetic resonance; Magnetic resonance angiography

AJNR Am J Neuroradiol 18:1463–1472, September 1997

Magnetic resonance (MR) angiography is widely used in the evaluation of intracranial aneurysms (1–4); however, the potential of MR angiography to show intracranial aneurysms is less than that of conventional angiography (1–4). The sensitivity for aneurysms measuring less than 5 mm in diameter is reported to be 55.6% to 56% and the sensitivity for aneurysms measuring 5 mm or larger in diameter is reported to be 86% to 87.5% (1, 2). Furthermore, MR angiography sometimes fails to depict giant aneurysms (5). The reasons for decreased signal in intracranial aneurysms are thought to be mainly slow and/or turbulent flow (6).

We studied the utility of MR angiography for the detection of aneurysms according to their type and the size of their necks. Specifically, our aim was to investigate the level of signal intensity in models of lateral and terminal saccular aneurysms with differing neck sizes and pulsatile flow with the use of three-dimensional time-of-flight (TOF) MR angiography with several imaging parameters, and to determine the effects that aneurysmal shape and imaging parameters have on their visibility.

Materials and Methods

Models and Flow Simulator (Fig 1)

Imaging was performed on a 1.5-T superconducting MR system with a commercially available head coil. A polytef tube with a 10-mm inside diameter was used as a vessel

Received July 15, 1996; accepted after revision March 13, 1997.

Supported in part by the Grant-in-Aid for Scientific Research (C) (No. 08671017) from the Ministry of Education, Science, Sports and Culture, Japan.

Presented in part at the annual meeting of the Japan Radiological Society, Tokyo, 1995.

From the Department of Radiology, Hamamatsu (Japan) University School of Medicine (H.I., Y.T., M.T., M.K.) and the Department of Radiology, University of Chicago (Ill) (H.I., R.G.R.).

Address reprint requests to Haruo Isoda, MD, Department of Radiology, Hamamatsu University School of Medicine, 3600 Handa-cho, Hamamatsu 431–31, Japan.

AJNR 18:1463–1472, Sep 1997 0195-6108/97/1808–1463

model. The lateral and terminal saccular aneurysm models were constructed of T-shaped or cross-shaped polytef connectors and one kind of polyolefin (Oyumarukun, Hinodewashi Inc, Tokyo, Japan). The height and fundus diameter of the models were 10 mm, and the neck diameter of both lateral (Fig 2) and terminal (Fig 3) saccular aneurysm models was 2.5 mm, 5 mm, 7.5 mm, and 10 mm, respectively. A parent artery model of each lateral saccular aneurysm model was placed in the z-axis (head to feet) direction in the MR scanner. Similarly, a parent artery model before the bifurcation of each terminal saccular aneurysm model was placed in the z-axis direction in the MR scanner. Only parent artery and aneurysm models were placed in the magnet.

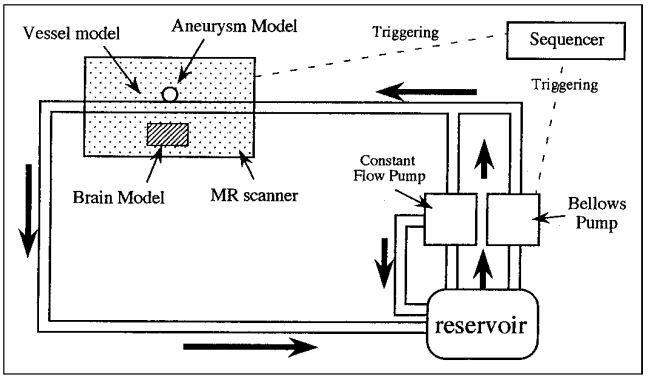

Fig 1. Diagram of the aneurysm models and flow simulator device. The sequencers control the bellows pump and pump out the fluid with a pulsation period of 1500 milliseconds. *Arrows* indicate the direction of flow.

At 1.4 T, T1 and T2 of blood is reported to be 1140 ± 54 milliseconds and 250 ± 18 milliseconds, respectively (7). Therefore, an aqueous solution of 1.0 mmol/L copper sulfate was used as the fluid, because its T1 is 1100 to 1200 milliseconds. We took care to make the T1 of this fluid mimic that of blood, because the T1 of the fluid was thought to affect the fluid's spin saturation. The T2 of the fluid was 150 to 200 milliseconds, which is less than that of blood; however, this was not thought to affect the experimental model.

The T1 relaxation times of deep gray matter and white matter are reported to be 1006 to 1223 milliseconds and 742 to 764 milliseconds, respectively (8). And T2 relaxation times of the same areas are reported to be 71 to 78 milliseconds and 73 to 77 milliseconds, respectively (8). Therefore, an aqueous solution of 1.25 mmol/L copper sulfate was used for the brain model, because its T1 is 820 to 900 milliseconds. We took care to make the T1 of the brain model mimic that of normal brain, because the T1 of the brain model was thought to affect the spin saturation. The T2 of the brain model was 160 to 180 milliseconds, which was somewhat greater than that of brain; however, this was again thought not to affect the experimental model. We used this solution as the "background" brain model when we evaluated the signal intensity of the intracranial aneurysm or vessel models.

A pulsatile flow generator was made of a bellows pump (Iwaki Bellows Pump Model KB-4N, Iwaki, Tokyo, Japan) and a constant flow pump (Nikkiso Magpon Model CP20-PPRV-10, Nikkiso Eiko, Tokyo, Japan), as shown in Figure 1. Two sequencers (Melsec-FX Model FX2–16MS and FX8EYT, Mitsubishi, Himeji, Japan) controlled the bellows pump and pumped the fluid with a pulsation period of

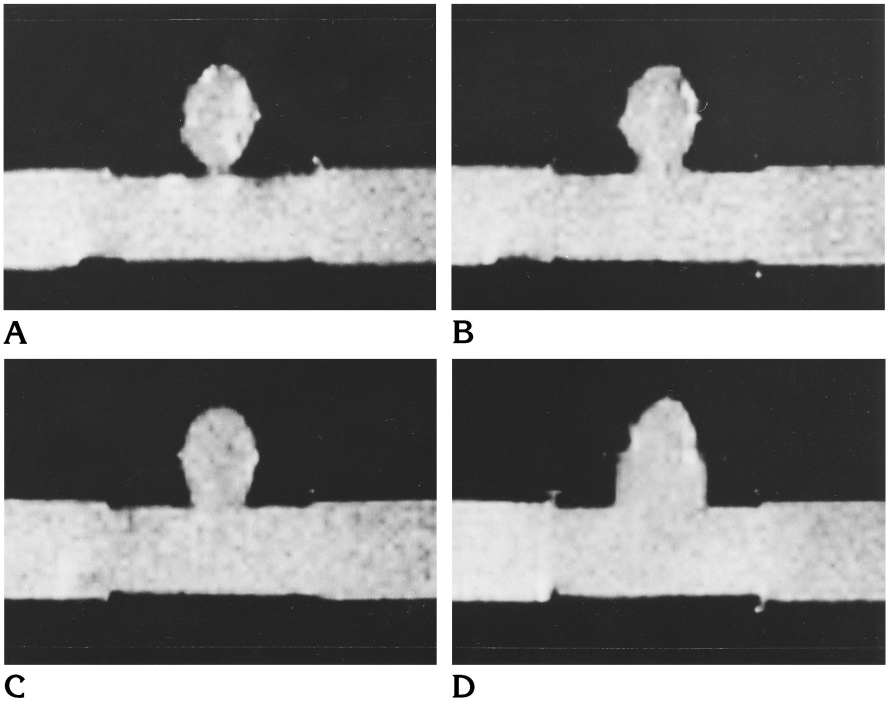

Fig 2. Spin-echo T1-weighted images (300/15) of lateral saccular aneurysm models with fluid but without active flow. The height and fundus diameter of the models were 10 mm; the neck diameters were 2.5 mm (*A*), 5.0 mm (*B*), 7.5 mm (*C*), and 10.0 mm (*D*).

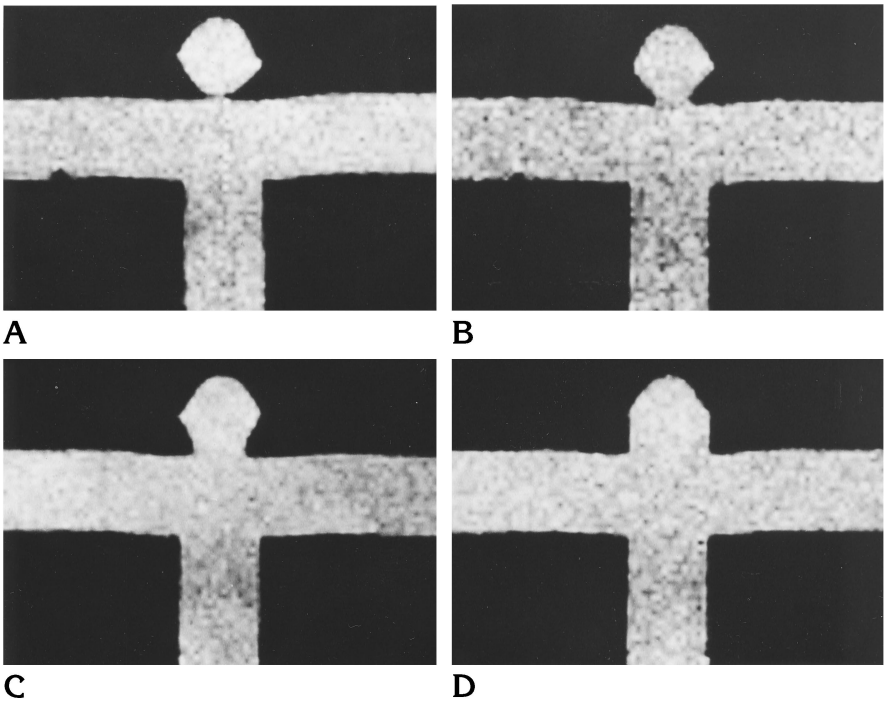

Fig 3. Spin-echo T1-weighted images (300/15) of terminal saccular aneurysm models with fluid but without active flow. The height and fundus diameter of the models were 10 mm; the neck diameters were 2.5 mm (*A*), 5.0 mm (*B*), 7.5 mm (*C*), and 10.0 mm (*D*).

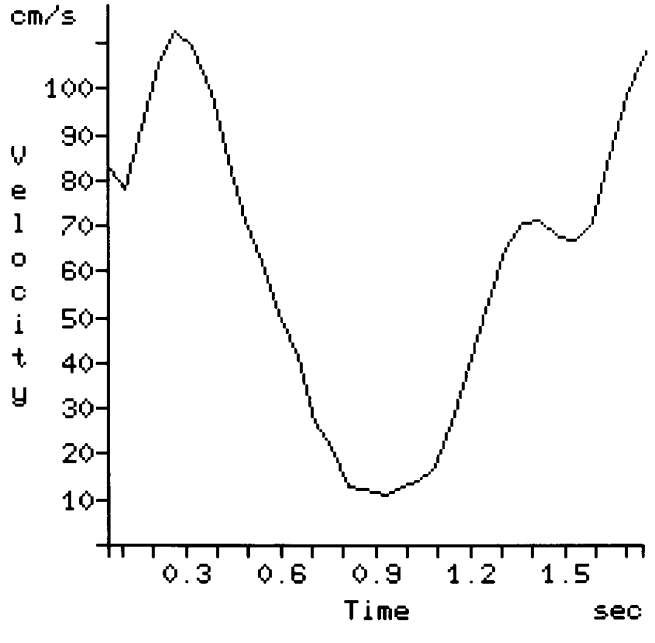

Fig 4. Fluid flow velocity curve as a function of time in the vessel models. A 2-D phase-mapping MR flow measurement was obtained for one pixel in the middle of the vessel models. Peak systolic velocity was about 110 cm/s and end-diastolic velocity was about 10 cm/s.

1500 milliseconds (Fig 4). The human internal carotid artery carries a volume of blood in an anterograde fashion during diastole; by sonography, the diastolic velocity is 30% to 40% of the peak flow during systole (9). Therefore, we used the constant flow pump in order to maintain flow during diastole, simulating the human internal carotid arteries. After adjusting the flow volume of each pump, we measured fluid flow velocity and its waveform using two-dimensional phase-mapping MR imaging (10). The electrocardiography (ECG)-triggering 2-D phase-mapping MR images were obtained using a fast low-angle shot with steady-state precession–type gradient-echo sequence with first-order flow compensation in the readout direction; imaging parameters were 34/6/1 (repetition time [TR]/echo time [TE]/excitations) flip angle of 20°, field of view (FOV) of 220 mm, acquisition matrix of 192 × 256, and section thickness of 6 mm. The ECG triggering was done by using sequencers (Fig 1). The velocity range was selected to keep the phase shift induced by the moving fluid at less than 360°. Images were acquired in an axial plane that was perpendicular to the parent vessel model in the lateral saccular aneurysm models or to the parent vessel model before the bifurcation in terminal saccular aneurysm models.

MR flow measurement of one pixel in the center of the vessel models showed that the peak systolic velocity was 110 cm/s, that end-diastolic velocity was 10 cm/s, and that mean velocity was 65 cm/s (Fig 4). MR flow measurement of whole pixels in vessel models showed that peak systolic velocity was 82 cm/s and that mean velocity was 47 cm/s. Fluid flow velocities and waveforms in our study were somewhat different from those in humans, but were thought to be superior to those of a constant flow model.

Data Acquisition

Three-dimensional TOF MR angiography was performed with flow-rephasing fast imaging with steady-state precession sequences with 20,40,60,80,100,120,140/7/1; flip angle of 10°, 20°, and 30°; slab thickness of 64 mm with 64 partitions; FOV of 128 mm; acquisition matrix of 128 × 128; and imaging time of 2 minutes 44 seconds to 19 minutes 7 seconds. A total of 21 sequences with different TRs and flip angles were obtained for each of the eight aneurysm models. When the lateral saccular aneurysm models were examined, the slabs were placed in the center of the models and in a transaxial direction, perpendicular to the parent vessel models. For the terminal saccular aneurysm models, the slabs were placed at the center of the necks and in a transaxial direction, perpendicular to the parent vessel models before the bifurcations.

Data Analysis

For the lateral saccular aneurysm models, regions of interest (ROIs) were placed on the original MR images that traversed the center of the aneurysms, and the signal intensity of all aneurysm models, parent vessel models, and background brain models was measured. For the terminal saccular aneurysm models, the ROIs were placed on the images that traversed the center of the aneurysms, and the signal intensity of the aneurysm models and background brain models was measured. Signal intensity of the parent vessel models on the images that traversed the parent vessel models before the bifurcations was also measured.

Although individual imaging parameters and imaging conditions, such as transmitter and receiver gain, were different, we did not standardize our data with such measurements as vessel-brain signal difference–to–noise ratios = (vessel signal intensity − brain signal intensity)/standard deviation of background noise (11), because we thought that this kind of standardization would reduce the information available from our data and make their tendencies and meanings unclear for this study. Therefore, we decided to evaluate absolute signal intensity. The signal intensity for the three flip angles used in the aneurysm models, parent vessel models, and background brain models, respectively, were plotted as a function of TR for each of the eight aneurysm models.

Results

With a TR of 40 or greater and a flip angle of 10°, there was little difference in signal intensity among the aneurysm models, vessel models, and background brain models, because transverse magnetization induced by an excitation pulse with a small flip angle was minimal (Figs 5, 6A and D, 7, and 8A and D). Signal intensity of vessel models was relatively strong at a TR of 20 and a flip angle of 10° (Figs 5 and 7). Furthermore, at a TR of 20 and a flip angle of 10°, the signal intensity of the terminal saccular aneurysm models with wider necks was almost isointense with that of the parent vessel models (Fig 7B–D).

The signal intensity of vessel models was stronger with larger flip angles (Figs 5–8). They were independent of TR at TRs of 60 or greater. The MR images that we used to measure the signal intensity were located at approximately the midportion of all imaging slabs, 30 mm away from the flowing fluid entry section in the slab. We estimated it took 60 milliseconds for the flowing fluid to reach the midsections from the entry point, because the mean flow velocity of the fluid was about 47 cm/s. Therefore, the signal intensity of the vessel models at TRs of 20 and 40 was decreased owing to spin saturation by several excitation pulses. Those at TRs of 60 or greater were independent of TR, because unsaturated fresh spins were exited. Reproducibility of the signal intensity was possible for all vessel models.

The signal intensity of brain models was greater with larger flip angles and/or greater TRs (Fig 5–8). Reproducibility of these signal intensities was possible for all models.

MR angiography with shorter TRs and/or larger flip angles showed weaker signal intensity in the aneurysm models than in parent arteries, because of spin saturation (Figs 5, 6B, 6E, 7, and 8B). We estimated that if the unsaturated fresh fluid had flowed into the aneurysm models and all the fluid in them had been replaced during the TR period, their signal intensity would have been the same as that in the parent vessel models. However, the signal intensity in the aneurysm models was observed to be less than that in the parent vessel models. The fluid spins in the aneurysm models were saturated, because these models decreased in signal intensity as a function of shorter TR (Figs 5 and 7). We further estimated that if fluid failed to flow into the aneurysm models, the signal intensity of these models would be less than that of the brain models, and their slopes would be less steep, because the T1 of fluid (1100 to 1200 milliseconds) was greater than that of the brain models (820 to 900 milliseconds). The signal intensity slopes for all aneurysm models were actually steeper than those for the brain models as a result of inflow of unsaturated fluid

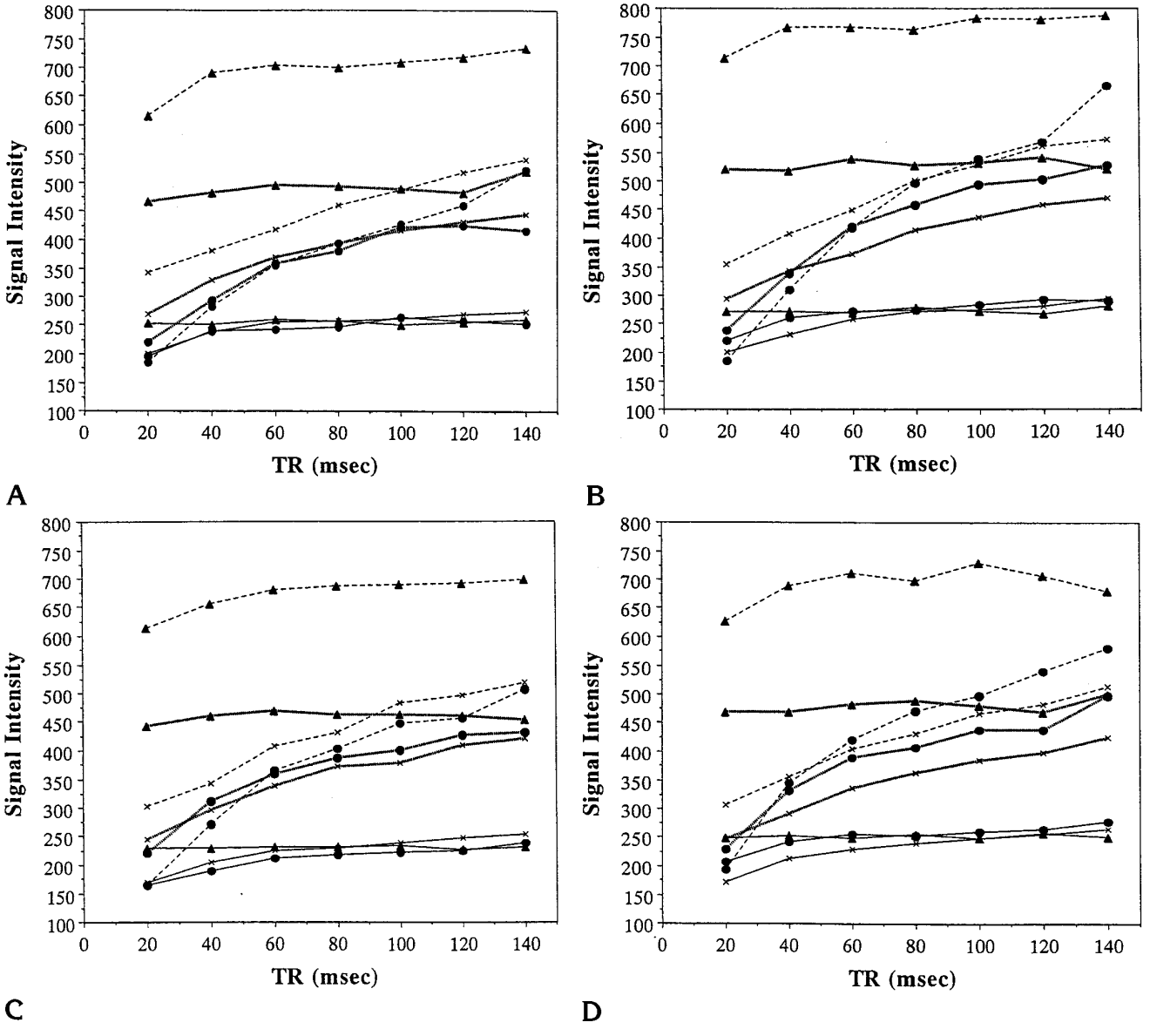

Key to Figure 5 (FA indicates degree of flip angle):

- FA=10, Brain Model
- FA=10, Aneurysm Model
- FA=10, Vessel Model
- FA=20, Brain Model
- FA=20, Aneurysm Model
- FA=20, Vessel Model
- FA=30, Brain Model
- FA=30, Aneurysm Model
- FA=30, Vessel Model

Fig 5. Signal intensity for each of three flip angles (10°, 20°, and 30°) of aneurysm models, parent vessel models, and background brain models is plotted as a function of TR (milliseconds) for each of four lateral saccular aneurysm models (neck diameter: *A*, 2.5 mm; *B*, 5.0 mm; *C*, 7.5 mm; *D*, 10.0 mm). There is little difference in signal among the models at a flip angle of 10°. Stronger signal intensity and greater slopes were obtained in aneurysm models with wider necks than in those with narrower necks. These findings were dependent on the flow. The aneurysm model with a neck of 7.5 mm (*C*) is an exception.

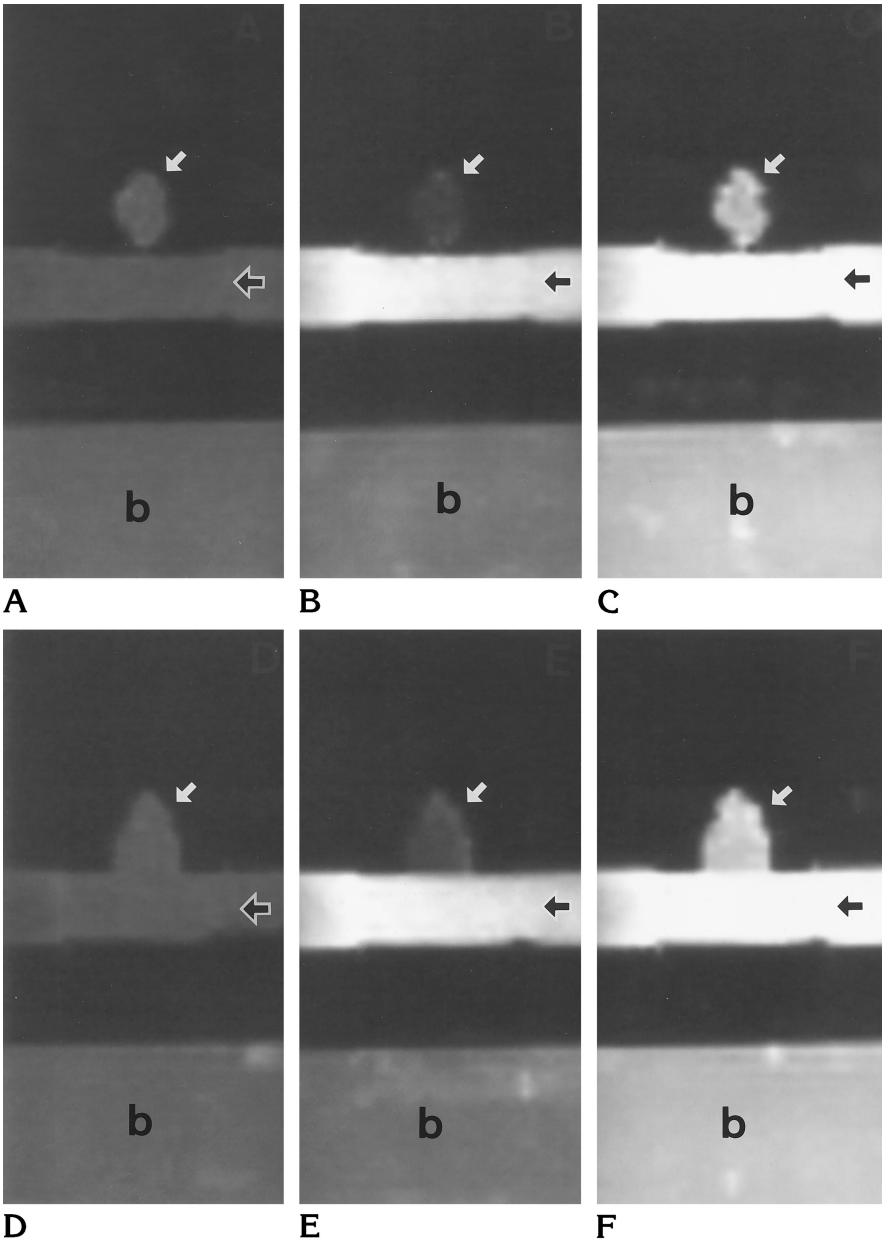

Fig 6. MR angiograms of lateral saccular aneurysm models with neck diameters of 2.5 mm (*A–C*) and 10.0 mm (*D–F*). All MR angiograms are displayed with the same window width and window center. *Black arrows* indicate flow direction in the parent vessel models.

A–C, Models with a neck size of 2.5 mm. There is little difference in signal among the aneurysm model (*white arrows*), the vessel model (*black arrows*), and the background brain model (*b*) in MR angiogram obtained with 120/7/1 and a 10° flip angle (*A*); however, the signal intensity is weak owing to small flip angle. In angiogram obtained with 20/7/1 and 30° flip angle (*B*), signal intensity in the vessel model is stronger. The background brain and aneurysm models have relatively weak signal intensity owing to short TR. Signal intensity in the aneurysm model is weaker than in the brain model, making aneurysm model hard to see. In angiogram obtained with 120/7/1 and 30° flip angle (*C*), the vessel and aneurysm models have stronger signal intensity than the background brain model. Signal intensity of the brain model is stronger with a flip angle of 30° (*C*) than with a flip angle of 10° (*A*). The vessel and brain models had stronger signal intensity at a TR of 120 (*C*) than at a TR of 20 (*B*).

D–F, Models with a neck size of 10 mm. There is little difference in signal among the aneurysm model (*white arrows*), the vessel model (*black arrows*), and the background brain model (*b*) in MR angiogram obtained with 120/7/1 and a 10° flip angle (*D*); however, the signal intensity is weak owing to small flip angle. In angiogram obtained with 20/7/1 and a 30° flip angle (*E*), signal intensity in the vessel model is stronger. The background brain and aneurysm models have relatively weak signal intensity owing to short TR. Signal intensity in the aneurysm model is weaker than in the brain model, making aneurysm model hard to see. In angiogram obtained with 120/7/1 and a 30° flip angle (*F*), the vessel and aneurysm models have stronger signal intensity than the background brain model (*b*).

into the aneurysm models (Figs 5 and 7). Therefore, in the aneurysm model, the degree of slope of the signal intensity and the signal intensity itself demonstrated the amount of unsaturated spins that flowed into the aneurysm models. Stronger signal intensity and greater slopes were obtained in the terminal saccular aneurysm models and/or models with wider necks than in the lateral saccular aneurysm models and/or models with narrower necks (Figs 5–8). These findings were thought to reflect the fact that the flow in the terminal saccular aneurysm models and/or models with wider necks was faster than the flow in the lateral saccular aneurysm models and/or models with narrower necks.

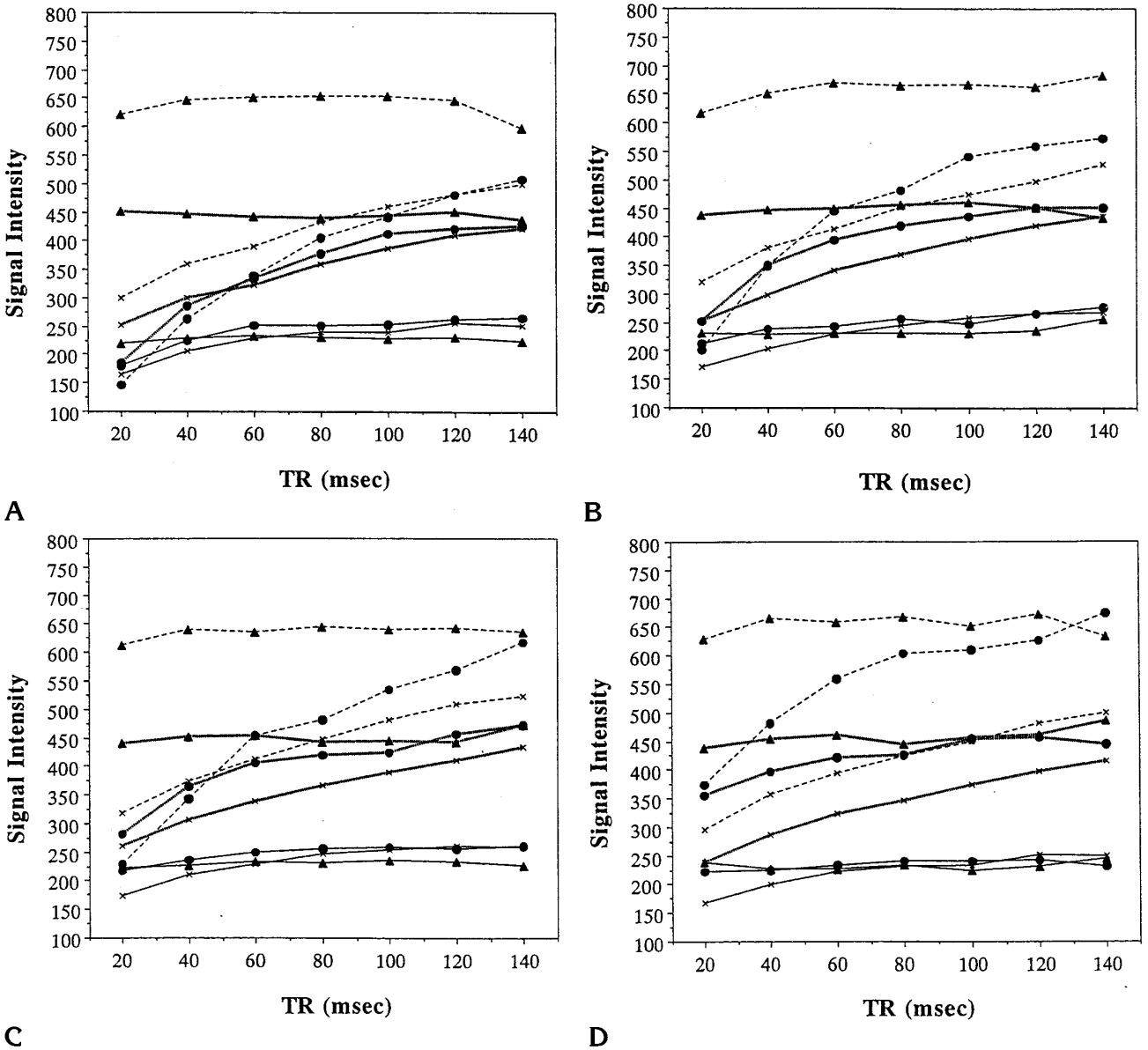

Key to Figure 7 (FA indicates degree of flip angle):

- FA=10, Brain Model
- FA=10, Aneurysm Model
- FA=10, Vessel Model
- FA=20, Brain Model
- FA=20, Aneurysm Model
- FA=20, Vessel Model
- FA=30, Brain Model
- FA=30, Aneurysm Model
- FA=30, Vessel Model

Fig 7. Signal intensity for each of three flip angles (10°, 20°, and 30°) of aneurysm models, parent vessel models, and background brain models is plotted as a function of TR (milliseconds) for each of four terminal saccular aneurysm models (neck diameter: *A*, 2.5 mm; *B*, 5.0 mm; *C*, 7.5 mm; *D*, 10.0 mm). There is little difference in signal among the models at a flip angle of 10°. Signal intensity of vessel models is stronger with larger flip angle and is independent of TR at TR of 60 or greater. Stronger signal intensity and greater slopes were obtained in aneurysm models with wider necks than in those with narrower necks. Signal intensity in each model was greater than that in lateral saccular aneurysms (Fig 5). These findings were dependent on the flow. However, there was little difference between the aneurysm with the 5.0-mm neck and that with the 7.5-mm neck.

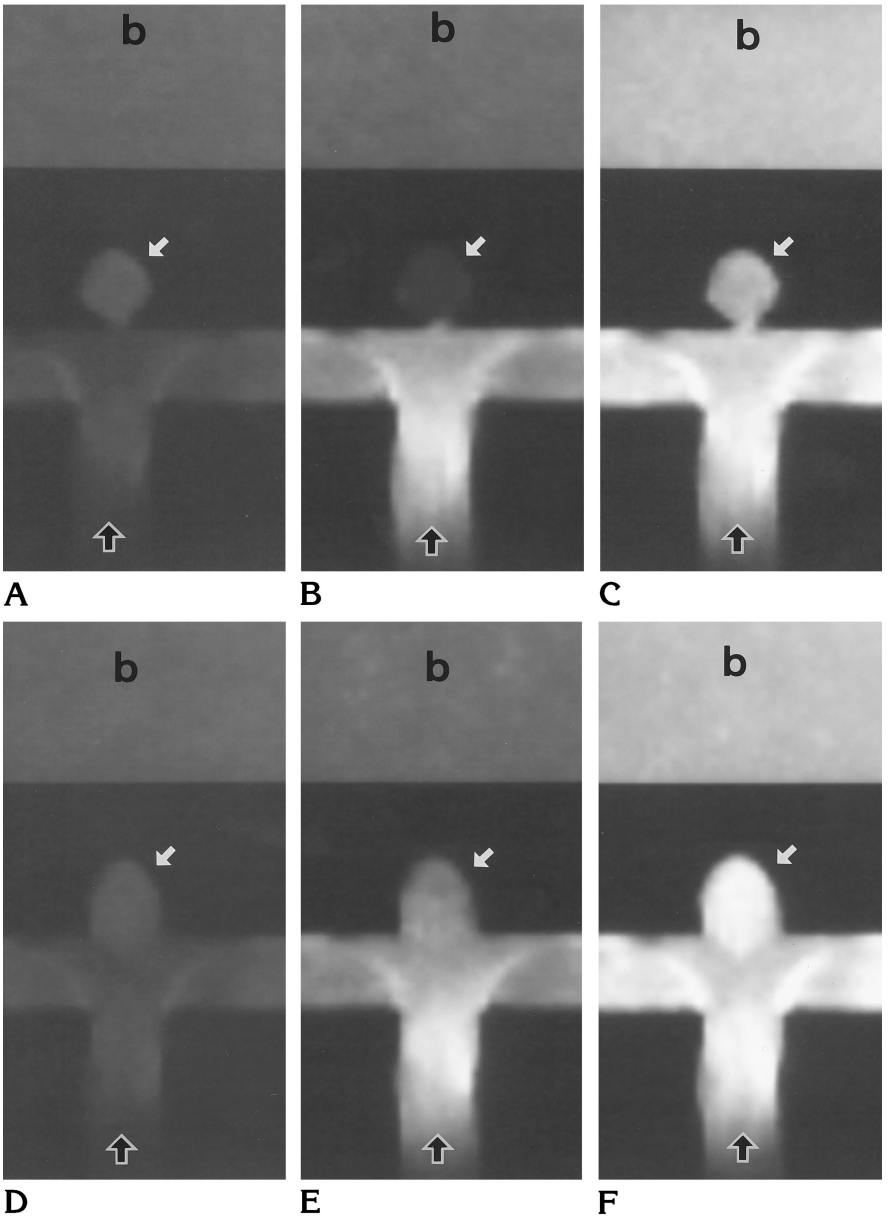

Fig 8. MR angiograms of terminal saccular aneurysm models with neck diameters of 2.5 mm (*A–C*) and 10 mm (D–F). The MR angiograms of the aneurysm models and background brain models were reconstructed separately with maximum intensity projection and are displayed in a row for each imaging sequences. All MR angiograms are displayed with the same window width and window center. *Black arrows* indicate flow direction in the parent vessel models.

A–C, Models with a neck size of 2.5 mm. There is little difference in signal among the aneurysm model (*white arrows*), the vessel model (*black arrows*), and the background brain model (*b*) in MR angiogram obtained with 120/7/1 and a 10° flip angle (*A*); however, the signal intensity is weak owing to small flip angle. In angiogram obtained with 20/7/1 and a 30° flip angle (*B*), signal intensity in the vessel model is stronger. The background brain and aneurysm models have relatively weak signal intensity owing to short TR. It is hard to see the aneurysm model, because it is weaker in signal intensity than the brain model. In angiogram obtained with 120/7/1 and a 30° flip angle (*C*), the vessel and aneurysm models have stronger signal intensity. The signal intensity of the brain model is stronger on the MR angiogram obtained with a flip angle of 30° (*C*) than on that with a flip angle of 10° (*A*). The vessel and brain models had stronger signal intensity at a TR of 120 (*C*) than at a TR of 20 (*B*).

D–F, Models with a neck size of 10 mm. There is little difference in signal among the aneurysm model (*white arrows*), the vessel model (*black arrows*), and the background brain model (*b*) in MR angiogram obtained with 120/7/1 and a 10° flip angle (*D*); however, the signal intensity is weak owing to small flip angle. In angiogram obtained with 20/7/1 and a 30° flip angle (*E*), the aneurysm and vessel models have relatively stronger signal than the background brain model owing to their rapid flow. Note the difference in signal intensity in the aneurysm model on this angiogram (*E*) compared with that in other aneurysm models (Figs 6B and E and 8B). In angiogram obtained with 120/7/1 and a 30° flip angle (*F*), the vessel and aneurysm models have stronger signal intensity than the background brain model.

Discussion

The possible reasons for decreased signal in intracranial aneurysms are thought to be related to slow and/or turbulent flow in the aneurysm (6). Vortex flow is also reported in aneurysms, and may contribute to their decreased signal intensity in some circumstances (12).

The results of our study indicate that 3-D TOF MR angiography with shorter TRs and larger flip angles is not optimal to see lateral or terminal saccular intracranial aneurysms because of spin saturation in them due to slow flow. Furthermore, the signal intensity in the aneurysms depends on the degree of unsaturated fluid flowing into them, the type of aneurysm, and the size of their neck. In general, terminal saccular aneurysms and/or aneurysms with wider necks were estimated to have stronger flow and greater signal intensity as compared with the lateral saccular aneurysms

and/or aneurysms with narrower necks. In particular, the terminal saccular aneurysm model with the widest neck showed hyperintense signal, even with a short TR (Fig 8E). Therefore, small basilar tip aneurysms with wider necks should be clearly seen. Other aneurysm models had lower signal intensity relative to the background brain model because the spins in these aneurysms were saturated. Terminal aneurysm models and/or aneurysm models with wider necks showed hyperintense signal relative to background brain models as a function of longer TR (Figs 5–8). Thus, 3-D TOF MR angiography with longer TRs should delineate aneurysms that are not visible at MR angiography with conventional parameters. In this situation, to shorten the time of acquisition, a reduced FOV and magnetic transfer contrast may be helpful (13).

Several of our aneurysm models did not show greater signal intensity relative to the background brain models as a function of a longer TR. In clinical situations, the use of contrast medium may help to solve this problem. Multiple thin slab 3-D TOF MR angiography (14) or 3-D TOF MR angiography with acetazolamide challenge (which increases cerebral blood flow) (15) may also be used to increase the detectability of intracranial aneurysms.

The flow or vortex in aneurysms is reported to vary according to their location, the size of their neck, and the flow volume of the parent vessels (16–19). In this study, the signal intensity of the aneurysm models with a neck size of 7.5 mm was somewhat less than that of aneurysms with a neck size of 5.0 mm. The reasons may be that the aneurysms with a 7.5-mm neck have a different vortex flow. The aneurysm models used in this study do not represent all kinds of intracranial aneurysms. Although we found no signal loss due to turbulence, this may have been a function of the models we used. Furthermore, the location of the aneurysms in the imaging slab was thought to play an important role in establishing the signal intensity in the aneurysm. Proximal aneurysms had a stronger signal intensity than distal ones, because spins flowing into the distal aneurysms were more saturated than those in proximal ones.

In summary, in our models, noncontrast 3-D TOF MR angiography showed terminal saccular aneurysms and/or aneurysms with wider necks better than lateral saccular aneurysms and/or aneurysms with narrower necks. Longer TRs are recommended to allow the spin flowing into the aneurysms to recover. Shorter TRs and larger flip angles were not optimal for seeing lateral or terminal saccular intracranial aneurysms.

Acknowledgment

We thank Yoshio Takemura for his assistance in making the pulsatile flow generator.

References

1. Korogi Y, Takahashi M, Mabuchi N, et al. Intracranial aneurysms: diagnostic accuracy of three-dimensional, Fourier transform, time-of-flight MR angiography. *Radiology* 1994;193:181–186
2. Huston J III, Nichols DA, Luetmer PH, et al. Blinded prospective evaluation of sensitivity of MR angiography to known intracranial aneurysms: importance of aneurysm size. *AJNR Am J Neuroradiol* 1994;15:1607–1614
3. Ronkainen A, Puranen MI, Hernesniemi JA, et al. Intracranial aneurysms: MR angiographic screening in 400 asymptomatic individuals with increased familial risk. *Radiology* 1995;195:35–40
4. Stock KW, Radue EW, Jacob AL, Bao X-S, Steinbrich W. Intracranial arteries: prospective blinded comparative study of MR angiography and DSA in 50 patients. *Radiology* 1995;195:451–456
5. Huston J III, Rufenacht DA, Ehman RL, Wiebers DO. Intracranial aneurysms and vascular malformations: comparison of time-of-flight and phase-contrast MR angiography. *Radiology* 1991;181:721–730
6. Bosmans H, Wilms G, Marchal G, Demaerel P, Baert AL. Characterization of intracranial aneurysms with MR angiography. *Neuroradiology* 1995;37:262–266
7. Mitchell MD, Kundel HL, Axel L, Joseph PM. Agarose as a tissue equivalent phantom material for NMR imaging. *Magn Reson Imaging* 1986;4:263–266
8. Breger RK, Yetkin FZ, Fischer ME, Papke RA, Haughton VM, Rimm AA. T1 and T2 in the cerebrum: correlation with age, gender, and demographic factors. *Radiology* 1991;181:545–547
9. Kerber CW, Liepsch D. Flow dynamics for radiologists. II. Practical considerations in the live human. *AJNR Am J Neuroradiol* 1994;15:1076–1086
10. Masui T, Isoda H, Mochizuki T et al. Effects of meal intake on the flow velocity in the superior mesenteric artery: evaluation with 2D phase mapping MRI. *J Comput Assist Tomogr* 1994;18:590–595
11. Edelman RR, Ahn SS, Chien D, et al. Improved time-of-flight MR angiography of the brain with magnetization transfer contrast. *Radiology* 1992;184:395–399
12. Strother CM, Graves VB, Rappe A. Aneurysm hemodynamics: an experimental study. *AJNR Am J Neuroradiol* 1992;13:1089–1095
13. Miyazaki M, Kojima F, Ichinose N, Onozato Y, Igarashi H. A novel saturation transfer contrast method for 3-D time-of-flight magnetic resonance angiography: a slice-selective off-resonance sinc pulse (SORS) technique. *Magn Reson Med* 1994;32:52–59
14. Davis WL, Warnock SH, Harnsberger HR, Parker DL, Chen CX. Intracranial MRA: single volume vs. multiple thin slab 3D time-of-flight acquisition. *J Comput Assist Tomogr* 1993;17:15–21
15. Mandai K, Sueyoshi K, Fukunaga R, et al. Acetazolamide challenge for three-dimensional time-of-flight MR angiography of the brain. *AJNR Am J Neuroradiol* 1994;15:659–665

16. Steiger HJ, Poll A, Liepsch D, Reulen H-J. Basic flow structure in saccular aneurysms: a flow visualization study. *Heart Vessels* 1987;3:55–65
17. Perktold K, Gruber K, Kenner T, Florian H. Calculation of pulsatile flow and particle paths in an aneurysm-model. *Basic Res Cardiol* 1984;79:253–261
18. Perktold K, Kenner T, Hilbert D, Spork B, Florian H. Numerical blood flow analysis: arterial bifurcation with a saccular aneurysm. *Basic Res Cardiol* 1988;83:24–31
19. Gonzalez CF, Cho YI, Ortega HV, Moret J. Intracranial aneurysms: flow analysis of their origin and progression. *AJNR Am J Neuroradiol* 1992;13:181–188